# $^{68}$Ga-DOTA-Tyr$^3$-Octreotide PET for Assessing Response to Somatostatin-Receptor–Mediated Radionuclide Therapy

Michael Gabriel[1], Andreas Oberauer[1], Georg Dobrozemsky[1], Clemens Decristoforo[1], Daniel Putzer[1], Dorota Kendler[1], Christian Uprimny[1], Peter Kovacs[2], Reto Bale[2], and Irene J. Virgolini[1]

*[1]Department of Nuclear Medicine, Innsbruck Medical University, Innsbruck, Austria; and [2]Department of Radiology, Innsbruck Medical University, Innsbruck, Austria*

$^{68}$Ga-labeled 1,4,7,10-tetraazacyclododecane-*N,N′,N′′,N′′′*-tetraacetic acid-D-Phe$^1$-Tyr$^3$-octreotide (DOTA-TOC) PET has proven its usefulness in the diagnosis of patients with neuroendocrine tumors. Radionuclide therapy ($^{90}$Y-DOTA-TOC or $^{177}$Lu-DOTA-octreotate) is a choice of treatment that also requires an accurate diagnostic modality for early evaluation of treatment response. Our study compared $^{68}$Ga-DOTA-TOC PET with CT or MRI using the Response Evaluation Criteria in Solid Tumors. Furthermore, standardized uptake values (SUVs) were calculated and compared with treatment outcome. **Methods:** Forty-six patients (29 men, 17 women; age range, 34–84 y) with advanced neuroendocrine tumors were investigated before and after 2–7 cycles of radionuclide therapy. Long-acting somatostatin analogs were not applied for at least 6 wk preceding the follow-up. Data were acquired with a dedicated PET scanner. Emission image sets were acquired at 90–100 min after injection. $^{68}$Ga-DOTA-TOC PET images were visually interpreted by 2 experienced nuclear medicine physicians. For comparison, multislice helical CT scans and 1.5-T MRI scans were obtained. Attenuation-corrected PET images were used to determine SUVs. Repeated CT evaluation and other imaging modalities, for example, $^{18}$F-FDG, were used as the reference standard. **Results:** According to the reference standard, $^{68}$Ga-DOTA-TOC PET and CT showed a concordant result in 32 patients (70%). In the remaining 14 patients (30%), discrepancies were observed, with a final outcome of progressive disease in 9 patients and remission in 5 patients. $^{68}$Ga-DOTA-TOC PET was correct in 10 patients (21.7%), including 5 patients with progressive disease. In these patients, metastatic spread was detected with the follow-up whole-body PET but was missed when concomitant CT was used. On the other hand, CT confirmed small pulmonary metastases not detected on $^{68}$Ga-DOTA-TOC in 1 patient and progressive liver disease not detected on $^{68}$Ga-DOTA-TOC in 3 patients. Quantitative SUV analysis of individual tumor lesions showed a large range of variability. **Conclusion:** $^{68}$Ga-DOTA-TOC PET shows no advantage over conventional anatomic imaging for assessing response to therapy when all CT information obtained during follow-up is compared. Only the development of new metastases during therapy was detected earlier in some cases when whole-body PET was used. SUV analysis of individual lesions is of no additional value in predicting individual responses to therapy.

**Key Words:** PET; radionuclide therapy; neuroendocrine; gallium-68; neuroendocrine tumors; peptide-related radionuclide therapy

**J Nucl Med 2009; 50:1427–1434**
DOI: 10.2967/jnumed.108.053421

Peptide-related radionuclide therapy (PRRT) is a new therapeutic procedure for patients with somatostatin receptor (SSTR)–positive tumors in advanced stages (*1,2*). This technique is based on the ability of tumor cells to overexpress SSTR, which can be targeted with radiolabeled analogs. Initial evaluation shows not only that a marked morphologic and biochemical response to therapy is observed but also that quality of life can be improved in many patients (*3*).

SSTR-positive neuroendocrine tumors (NET) originated in the gastrointestinal tract and the lung in most cases (*4,5*). However, various other non-NET cancers, for example, sarcomas (*6*), can also show a high level of uptake on SSTR scintigraphy, as is a prerequisite for effective treatment. If patients have access to PRRT, therapy response is superior to that with the current treatment scheme for NET (*7*).

A recent study on 84 patients showed that $^{68}$Ga-labeled 1,4,7,10-tetraazacyclododecane-*N,N′,N′′,N′′′*-tetraacetic acid-D-Phe$^1$-Tyr$^3$-octreotide (DOTA-TOC) PET is useful in the diagnosis of NET, showing greater efficacy than that obtained with conventional scintigraphy and diagnostic CT alone (*8*). Furthermore, some of these patients were successfully selected to receive PRRT on the basis of significant tracer uptake. Patients were selected for treatment with $^{90}$Y-DOTA-TOC or $^{177}$Lu-DOTA-octreotate (DOTATATE) according to individual lesion size (*9*).

In clinical routine, radiologic imaging techniques are well established for the evaluation of response after therapy. For solid tumors, assessment of therapy response is

Received Apr. 13, 2008; revision accepted May 15, 2009.
For correspondence or reprints contact: Michael Gabriel, Department of Nuclear Medicine, Innsbruck Medical University, Anichstrasse 35, 6020 Innsbruck, Austria.
E-mail: michael.gabriel@i-med.ac.at

based on the Response Evaluation Criteria in Solid Tumors (RECIST), which define response as a 30% decrease in the largest diameter of the tumor (*10*). RECIST criteria do not seem to be the best choice for evaluating therapy response in NET. However, several guidelines recommend the use of CT and MRI for initial diagnosis and follow-up of these tumors (*11*).

These tumors are generally rather heterogeneous in terms of pathologic differentiation and biologic behavior, as is also expressed by varying values on the proliferation index. Besides the variety of tumor characteristics, the different pharmacologic and physical properties of the radiopharmaceuticals used should also be considered when one is evaluating therapy response. Internal radiation therapy induces damage to tumor cells during a longer period because of the high-energy β-emitter $^{90}$Y or the medium-energy β-emitter $^{177}$Lu. Consequently, some degree of necrosis will continuously accumulate, and on subsequent examination the presence of necrotic and fibrotic tissue may cause the size of lesions to appear unchanged. This problem requires new response-evaluation techniques.

The aim of this study was to evaluate the usefulness of visual evaluation of therapy-induced changes in tumor uptake for early prediction of tumor response using $^{68}$Ga-DOTA-TOC PET. For visual interpretation during follow-up, $^{68}$Ga-DOTA-TOC was compared with diagnostic CT and MRI. Moreover, a quantitative analysis of the baseline and posttherapy $^{68}$Ga-DOTA-TOC PET scans was performed, because an increased standardized uptake value (SUV) at baseline has been shown to be associated with increased receptor binding, indicating a favorable therapeutic effect (*12*).

## MATERIALS AND METHODS

From August 2004 to December 2006, a total of 46 consecutive patients (29 men, 17 women; age range, 34–84 y; mean age ± SD, 59.2 ± 11.7 y) with advanced tumors having enhanced SSTR expression were included in this investigation.

The tumors originated in neuroendocrine tissue of the gastrointestinal tract in 41 patients. In addition, 3 patients with a carcinoid tumor of the lung, 1 patient with a glomus tumor, and 1 patient with a dendritic reticulum cell sarcoma with metastases in the regional lymph nodes were included. The patients were scanned before radionuclide therapy and after 2–7 cycles thereof. Restaging was done within a range of 34–120 d (mean, 77 d; SD, 23.8 d) from the last therapy cycle. Long-acting somatostatin analogs were not administered for at least 6 wk before the follow-up PET scan.

Various therapeutic procedures were performed before inclusion in the study. Most of the patients were treated surgically ($n$ = 42). Thirty-five patients received additional drug therapy after surgery and before inclusion in the study; 9 patients received chemotherapy, and 26 received long-acting somatostatin analogs alone or in combination with interferon-α. Seven patients were treated with surgery alone, and 4 patients who had advanced disease at initial staging were treated with chemotherapy alone.

Twenty-four patients were consecutively treated with $^{90}$Y-DOTA-TOC, 19 with $^{177}$Lu-DOTA-TATE, and 3 with both compounds. Uptake on the pretherapy $^{68}$Ga-DOTA-TOC PET scans was scored visually. Inclusion in this study required a higher uptake in the tumor than in normal liver tissue. Details of patient characteristics are shown in Supplemental Table 1 (supplemental materials are available online only at http://jnm.snmjournals.org).

Written informed consent was obtained from all patients before they were enrolled in the study, and repeated administration of $^{68}$Ga-DOTA-TOC PET was approved by the local ethics committee.

### PET Tracer Preparation, Data Acquisition, and Processing

$^{68}$Ga-DOTA-TOC was prepared using a fully automated method for preparation of $^{68}$Ga-labeled peptides as described by Decristoforo et al. (*13*).

Patient imaging and image reconstruction were performed on a dedicated PET scanner (Advance; GE Healthcare) as described previously (*8*), with acquisition 90–100 min after injection of 100–150 MBq. The acquisition time was chosen on the basis of SUV calculations from serial imaging (*8*).

Attenuation-corrected $^{68}$Ga-DOTA-TOC PET images were used to determine SUV. Irregular isocontour regions of interest were drawn over the target lesion at 50% of maximum pixel value within the tumor. The individual patient's region of interest was placed in the same target lesion on the pre- and posttherapy $^{68}$Ga-DOTA-TOC PET scans for quantitative intrapatient comparison. SUV was calculated using the maximum activity values in the region of interest normalized for the injected dose and patient body weight.

### CT and MRI

For comparison, 2.5-mm helical CT was performed on a HiSpeed CT/i Advantage scanner (GE Healthcare). Typically, approximately 150 mL (2 mL/kg of body weight) of Visipaque 320 contrast medium (GE Healthcare) were administered. MRI was performed on a 1.5-T whole-body scanner (Magneton Vision; Siemens Medical Systems) using a phased-array surface coil. T1- and T2-weighted spin-echo images were obtained with and without fat suppression.

### Evaluation Protocol

All patients underwent CT before and at the end of the study; these scans were obtained in parallel with $^{68}$Ga-DOTA-TOC PET scans according to the study protocol, as shown in Figure 1.

Diagnostic CT and, if indicated, MRI and whole-body $^{68}$Ga-DOTA-TOC PET were performed within the 3 wk preceding initial therapy for baseline evaluation. The interval between $^{68}$Ga-DOTA-TOC PET and CT ranged from 2 to 5 d. Patients received radionuclide therapy according to our protocol, as described elsewhere (*9*).

After the last therapy cycle, each patient underwent follow-up with $^{68}$Ga-DOTA-TOC PET and CT of the neck, chest, and abdomen. In 1 patient with a dendritic reticulum sarcoma, an MRI scan of the head and neck was available.

### Reference Standard

Validation of findings was based on repeated CT of the chest and abdomen at 3- to 6-mo intervals during the first year after initial restaging with $^{68}$Ga-DOTA-TOC PET and concomitant CT.

Besides the course of disease as assessed by repeated CT, in some cases complementary imaging modalities such as lesion-guided MRI, $^{18}$F-fluoride and $^{18}$F-FDG PET, endoscopy, and ultrasonography were also used for earlier evaluation of the

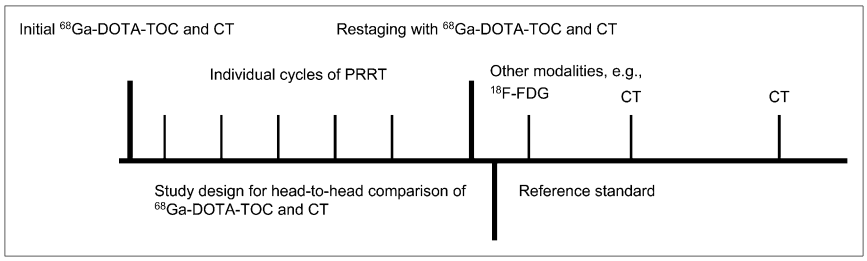


**FIGURE 1.** Schedule of PRRT evaluation study performed with CT and $^{68}$Ga-DOTA-TOC. Head-to-head analysis of PET and CT was based on comparison of initial scan with posttherapy scan. Final verification was obtained with reference standard.

outcome of radionuclide therapy, especially when unexpected $^{68}$Ga-DOTA-TOC PET findings were of clinical relevance.

### Interpretation and Data Analysis

$^{68}$Ga-DOTA-TOC PET data were independently interpreted by 2 experienced nuclear medicine specialists. For the visual response assessment, the baseline and follow-up $^{68}$Ga-DOTA-TOC PET data were compared side by side by the 2 specialists. If their findings were discordant, a third reader was consulted, who acted as referee. All readers were aware of the patient's clinical history but were unaware of any result of other imaging modalities.

Typically, axial, coronal, and sagittal images and maximum-intensity-projection images for review in the 3-dimensional cine mode were available.

$^{68}$Ga-DOTA-TOC PET images were analyzed for the presence of focal lesions with increased tracer uptake. Lesions were interpreted as metastases if their uptake was greater than uptake in the surrounding background tissue and if, thus, a focal lesion was clearly depicted.

The longest diameter of the index lesion at various sites on the $^{68}$Ga-DOTA-TOC PET scans was used to measure the course of disease. According to RECIST criteria, only measurable lesions (i.e., those that can be accurately measured in at least 1 dimension) 10 mm or more in longest dimension were target lesions in this study. The regions of interest for the PET images were assigned by the second author for determination of diameter and SUV.

The size of $^{68}$Ga-DOTA-TOC PET lesions was determined by semiquantitative assessment. First, the maximal SUV of the lesion was determined. Then, a threshold of half the maximum was applied to the display, and the portion of the lesion above the threshold was measured as the lesion size. A size decrease of more than 30% in the largest lesion and disappearance of preexisting measurable lesions at various other sites, without the appearance of any new abnormal findings, was deemed disease regression. When the pretherapy and posttherapy $^{68}$Ga-DOTA-TOC PET scans were compared, an increase of more than 20% in the longest diameter of a lesion after completion of therapy was deemed disease progression. A finding of new lesions on the whole-body $^{68}$Ga-DOTA-TOC PET scan after therapy was considered to indicate progressive disease regardless of any changes in the size of the index lesion. In all other cases, no significant change was assumed, that is, stable disease.

CT and, if necessary, MRI scans were interpreted by experienced radiologists who had no knowledge of the scintigraphy results or of clinical data. They compared the CT findings before and after therapy side by side. In the case of interobserver differences, a third reader was also consulted, who acted as referee. The PET readers did not also read the CT scans.

RECIST was used for CT and MRI in determining radiographic tumor response to treatment (*10,11*).

The $^{68}$Ga-DOTA-TOC PET and CT findings were categorized as response to therapy, stable disease, or progressive disease. Complete response, minor response (i.e., tumor shrinkage of $<$30%), and partial response were combined to form a single category after posttherapy CT evaluation.

After a masked and independent evaluation of the $^{68}$Ga-DOTA-TOC PET and CT data, the results were consecutively compared and classified as matching or mismatching. A definitive decision on the success of therapy was based on the reference standard, as previously mentioned.

Additionally, SUV or relative changes in SUV were analyzed for the target lesion on $^{68}$Ga-DOTA-TOC PET, which was most visible and easy to define. Quantitative analysis was performed without knowledge of the outcome of the visual PET evaluation. For assessment of SUV efficacy, individual quantitative data were assigned to clinical outcome, as assessed with the reference standard.

### Statistical Analysis

The McNemar test of correlated properties was used to statistically compare the imaging results for $^{68}$Ga-DOTA-TOC PET and corresponding CT on a patient-by-patient basis. Cohen's $\kappa$ with confidence intervals of 95% was used to demonstrate the degree of association. The $\chi^2$ test for independence was used to evaluate differences in subgroups when patients treated with $^{177}$Lu-DOTA-TATE were compared with those treated with $^{90}$Y-DOTA-TOC.

All quantitative data are presented as mean $\pm$ SD. The difference in SUV on the pretherapy scans between clinical responders, patients with stable disease, and nonresponders was tested with the Mann–Whitney *U* test, which was also used to assess statistical differences in terms of percentage change during therapy. Percentage change was calculated from SUV before and SUV after as follows: (SUV before $-$ SUV after) $\times$ 100/SUV before. For paired comparisons of patients (e.g., before and after PRRT), the Wilcoxon signed-rank test was used. All tests were 2-sided and performed at the 5% level of significance.

## RESULTS

The follow-up period after PRRT ranged from 57 to 556 d (mean, 337 d). During the follow-up period, 12 patients died. Seven patients died from tumor disease (patients 7, 9, 14, 17, 20, 30, and 40). One 84-y-old patient (patient 2) died from severe impairment of renal function. Furthermore, patient 6 died from acute myeloblastic leukemia, patient 16 from cerebral hemorrhage, patient 28 from pneumonia, and patient 29 from a grand mal seizure.

According to the reference standard, 14 (30%) of the 46 patients had a documented remission, including 4 (9%) patients with a minor response, 9 (20%) with a partial response, and 1 (2%) with a complete response. In this

patient (patient 31), multiple small liver metastases of a carcinoid tumor of the rectum completely disappeared after 4 cycles of $^{177}$Lu-DOTA-TATE. Twenty-two patients (48%) showed stable disease, and 10 patients (22%) progressive disease.

Progressive disease was documented at various sites: bone (patients 6 and 14), liver (patients 7, 9, and 17), lung (patient 11), bone and liver (patients 20, 30, and 40), and bone and lung (patient 25). Mixed responses were not observed during follow-up using radiologic criteria for CT evaluation. However, morphologic signs of necrosis in index lesions were frequently found in liver metastases during CT follow-up.

### Head-to-Head Comparison of $^{68}$Ga-DOTA-TOC PET and Concomitant Diagnostic CT

According to the applied response criteria as described in the "Materials and Methods," a concordant result between $^{68}$Ga-DOTA-TOC PET and early CT reevaluation was observed in 32 patients (70%), including 1 patient with progression, 22 (48%) with stable disease, and 9 (19%) with remission. All these conclusive results turned out to be correct. The remaining 14 patients (30%) showed discrepancies, including 9 patients (19%) with progressive disease and 5 (11%) with remission to therapy. Here, $^{68}$Ga-DOTA-TOC PET was superior to CT in 10 patients (22%), including 5 with progressive disease; that is, patients 6 and 20 showed additional bone metastases, as seen in Figure 2. In patients 7 and 14, additional liver metastases were observed on the follow-up scan, and in patient 40 with a NET of the pancreas (vasoactive intestinal polypeptide-secreting tumor), additional liver and bone metastases were observed on the follow-up scan. In 5 patients, PET demonstrated only response to therapy, as shown in Figure 3, including 4 patients with a partial response (patients 8, 15, 16, and 19) and 1 patient with a minor response (patient 28).

By contrast, diagnostic CT was superior to $^{68}$Ga-DOTA-TOC PET in 4 patients (patients 9, 11, 17, and 30), all of whom showed progressive disease. In patient 11, small pulmonary metastases not detected with $^{68}$Ga-DOTA-TOC developed, whereas the other 3 patients (patients 9, 17, and 30) showed a decrease in tracer uptake at tumor sites in the liver during therapy because of an advanced dedifferentiation process but enhanced $^{18}$F-FDG accumulation, revealing a flip-flop phenomenon (*14*). These 3 patients died from tumor progression within 1 y after restaging.

When the diagnostic efficacy of $^{68}$Ga-DOTA-TOC PET and CT was compared at early finalization of PRRT, $^{68}$Ga-DOTA-TOC showed higher diagnostic efficacy than did CT according to visual response criteria. However, the difference was not statistically significant on the McNemar test ($P = 0.27$). Cohen's κ of 0.47 demonstrated moderate agreement between the 2 modalities.

When subgroups of patients treated with either $^{177}$Lu-DOTA-TATE ($n = 20$) or $^{90}$Y-DOTA-TOC ($n = 23$) were compared, no statistically significant difference was observed ($P = 0.78$) with regard to the efficacy of $^{68}$Ga-DOTA-TOC for assessing PRRT.

### Use of Lesion Diameter to Predict Therapy Response with $^{68}$Ga-DOTA-TOC

In 16 patients, individual target lesions disappeared or decreased significantly in size, indicating remission to therapy. In addition to those 14 patients who were later confirmed as responders to therapy, a significant decrease of the index lesion on the $^{68}$Ga-DOTA-TOC PET scan was also found in 2 patients with progressive disease (patients 7 and 9). However, most patients showed no significant change in the index lesion. More details on changes in lesion diameter and correlation with long-term outcome are given in Table 1.

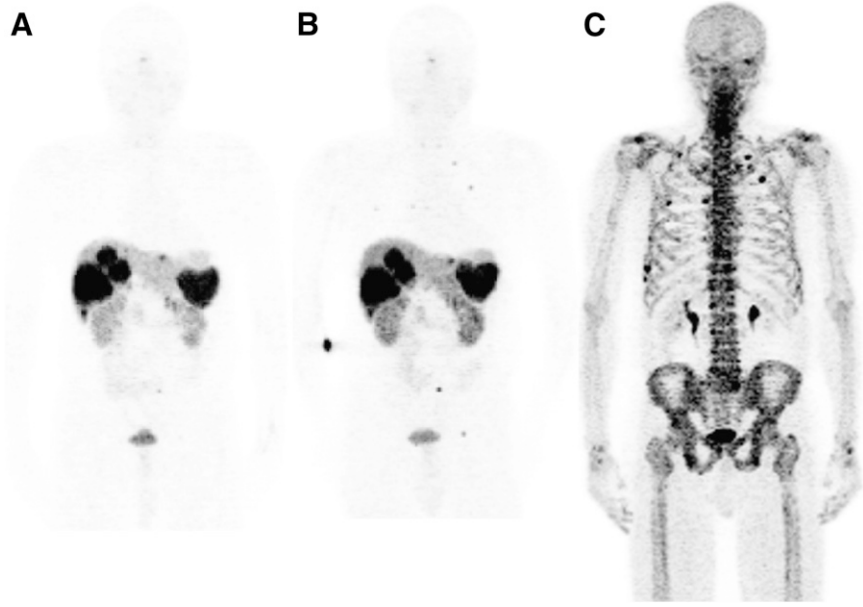


**FIGURE 2.** A 59-y-old man with multiple liver metastases of gastrinoma as shown in pretreatment scan (A). Because uptake in these large lesions was high, patient was given 4 cycles of $^{90}$Y-DOTA-TOC. However, follow-up scan additionally showed multiple small bone metastases (B) not detected by CT, which were confirmed by $^{18}$F-fluoride PET (C).

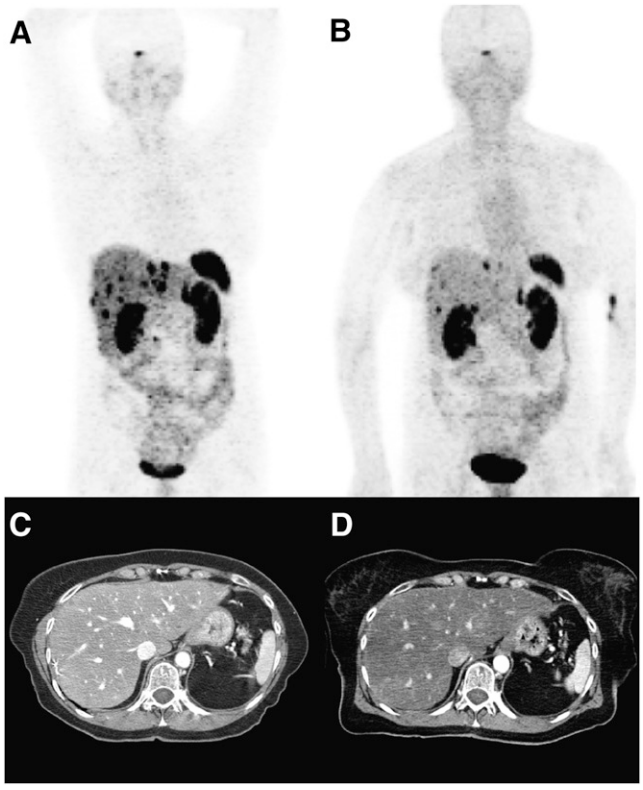


**FIGURE 3.** A 55-y-old woman with multiple small liver metastases (A). After surgical resection of primary tumor in pancreatic head, 4 cycles of $^{177}$Lu-DOTA-TATE were applied. Excellent treatment response was observed in $^{68}$Ga-DOTA-TOC PET scan (B). However, corresponding CT scans initially showed no remarkable change in liver lesions (C and D).

Because the study protocol required masked analysis of each modality, different target lesions were frequently selected for PET and CT evaluation. Considering the widespread metastatic disease in most of the study population, head-to-head correlation of anatomic and PET-based size parameters of index lesions was possible for only 2 patients (patients 21 and 29) with a large solitary target lesion in the neck. One of these 2 patients had a glomus tumor (patient 21), and the other had a dendritic reticulum cell sarcoma (patient 29), with neither CT nor PET showing a change in size after therapy.

### Whole-Body PET Evaluation with $^{68}$Ga-DOTA-TOC

On the $^{68}$Ga-DOTA-TOC whole-body PET scan, metastatic spread of tumor lesions was observed in 6 (13%) of 46 patients after finalization of PRRT, which was also confirmed by the reference standard. In 5 patients (patients 6, 7, 14, 20, and 40), as already mentioned, abnormal findings were observed on $^{68}$Ga-DOTA-TOC PET but were missed on the corresponding CT performed at the same time.

### Quantitative Evaluation of $^{68}$Ga-DOTA-TOC and Correlation with Response to PRRT

One patient (patient 34) was excluded from SUV calculation because of defective transmission data in the follow-up scan. SUV for the initial PET scan ranged from 6.4 in patient 38, showing stable disease after therapy, to 267 in patient 45, who was referred for treatment of a small-bowel carcinoid. This patient showed a minor response after therapy.

Concerning evaluation of the baseline $^{68}$Ga-DOTA-TOC PET scan, no significant difference in tumor SUV was observed between patients subsequently defined as responders to therapy and patients showing progressive disease after finalization of therapy ($P = 0.12$). However, a significant difference in SUV was indeed observed when responders were compared with patients with stable disease ($P = 0.031$) or with the total number of patients with stable disease or progressive disease ($P = 0.028$).

The relative decrease in $^{68}$Ga-DOTA-TOC uptake during therapy, that is, the change from the pre- to posttherapy scans, was also markedly higher for patients showing a response to therapy ($-38\% \pm 40\%$ in responders) than for patients with stable disease ($-3.1\% \pm 42\%$ in stable disease; $P = 0.031$) or nonresponders ($-5.4\% \pm 46\%$ in nonresponders; $P = 0.12$). However, Figure 4 shows considerable mean variation and overlap in the relationship between clinical response and changes in $^{68}$Ga-DOTA-TOC parameters, as can also be found in Table 2 using a cutoff level of $\pm 20\%$.

In addition to the cluster-specific SUV evaluation, further intrapatient analysis was performed to show a possible relationship between clinical response, as assessed by the reference standard, and the individual changes in $^{68}$Ga-DOTA-TOC uptake as a surrogate marker of SSTR expression. However, this analysis shows that the intraindividual quantitative parameters changed rather randomly, as shown in Figure 5.

## DISCUSSION

PRRT can be considered for patients with inoperable metastatic disease and positive SSTR findings. Although several studies have shown promising overall results,

**TABLE 1.** Correlation of Diameter of Index Lesion on $^{68}$Ga-DOTA-TOC PET and Long-Term Outcome

| Results in terms of lesion size | Remission ($n = 14$) | Stable disease ($n = 22$) | Progressive disease ($n = 10$) |
|---|---|---|---|
| Increase (≥20%) | 0 | 0 | 0 |
| No significant change | 0 | 22 | 8 |
| Decrease (>30%) | 14 | 0 | 2 |

Data are number of patients. Remission, stable disease, and progressive disease were as assessed according to reference standard.

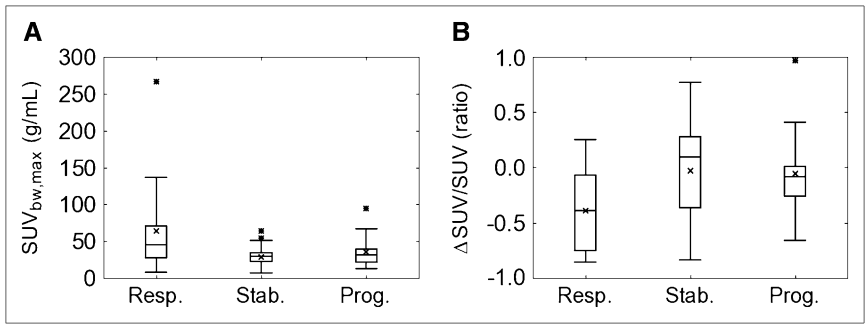


**FIGURE 4.** Comparison of SUV and changes according to objective response criteria. (A) Differences in $^{68}$Ga-DOTA-TOC uptake ($SUV_{bw,max}$) on first PET scan are shown for responders, patients with stable disease, and nonresponders. Box plots show range from first to third quartiles as box, median as horizontal line, and mean as x. Whiskers denote minimum data range or 1.5 interquartile ranges. Outliers are denoted by stars. (B) Change in uptake at tumor sites (maximal SUV) is expressed as ratio of pretreatment to posttreatment scans according to treatment outcome. Progr. = progressive disease; resp. = responder to therapy; stab. = stable disease; $SUV_{bw,max}$ = maximal SUV normalized for body weight.

reported antitumor effects vary considerably in the literature (*2,15–19*). Besides standardization of the therapy protocol, adequate methods for assessing therapy response are required.

To our knowledge, this was the first study to describe the value of $^{68}$Ga-DOTA-TOC PET for assessing radionuclide therapy in patients with SSTR-positive tumors. In our setting, $^{68}$Ga-DOTA-TOC PET was used not only as a baseline scan for therapy selection but also as a follow-up scan for patients after therapy.

### Overall Efficacy of $^{68}$Ga-DOTA-TOC PET Using RECIST Criteria

Although $^{68}$Ga-DOTA-TOC PET showed results concordant with the reference standard in 42 (91%) of 46 patients, false results were obtained in 4 patients, including 1 woman in whom small pulmonary metastases developed during therapy. Small pulmonary lesions can escape detection by nuclear medicine techniques because of their limited spatial resolution as compared with anatomically oriented methods (*20*). Therefore, contrast-enhanced multislice CT can be considered an essential imaging method for the evaluation of NET (*21*).

CT was also useful in 3 other patients showing discrepant findings for $^{68}$Ga-DOTA-TOC PET and CT. In these patients, the change of the target lesion did not indicate progressive disease, nor were any further tumor lesions identified by whole-body PET, whereas diagnostic CT clearly showed progressive disease in the form of extensive liver involvement. Solitary liver lesions even lost their receptor binding ability for $^{68}$Ga-DOTA-TOC. Because $^{18}$F-FDG PET showed enhanced uptake in these $^{68}$Ga-DOTA-TOC–negative lesions, further tumor dedifferentiation was assumed (*22,23*), as shown in Figure 6. Although $^{18}$F-FDG PET is normally of limited value in evaluating well-differentiated NET, in these 3 patients it provided further information on outcome. All patients with $^{18}$F-FDG PET–positive/$^{68}$Ga-DOTA-TOC–negative findings died from tumor progression within several months. Whether $^{18}$F-FDG also has a prognostic value in view of this fact remains to be further clarified.

Despite correct findings in patients showing a response to therapy, the fact that no significant size change was found in most patients indicates that evaluation of individual lesions on $^{68}$Ga-DOTA-TOC PET is a poor predictor of progressive disease. A decrease in the diameter of the index lesion was observed even in 2 patients with progressive disease. New, unexpected distant metastases were identified on posttherapy whole-body PET in 1 of these patients. These contradictory findings lead us to conclude that lesion-based analysis cannot be recommended as a means of predicting individual therapy response.

On the other hand, $^{68}$Ga-DOTA-TOC was found to be a useful complement to morphologically oriented methods for the early assessment of progressive disease after finalizing PRRT, namely in that it detects new, still undiscovered lesions on whole-body PET. In 5 patients, progressive disease was depicted even somewhat earlier than with other methods. In particular, PET has proven to be a sensitive means of detecting new bone lesions and might even have value for further clinical management (*24*).

**TABLE 2.** Correlation of Maximal SUV of Index Lesion on $^{68}$Ga-DOTA-TOC PET and Long-Term Outcome

| Results in terms of ΔSUV | Remission ($n$ = 13) | Stable disease ($n$ = 22) | Progressive disease ($n$ = 10) |
|---|---|---|---|
| Increase (≥20%) | 1 | 7 | 2 |
| No significant change (<20%) | 4 | 7 | 5 |
| Decrease (≥20%) | 8 | 8 | 3 |

Data are number of patients. Remission, stable disease, and progressive disease were as assessed according to reference standard.

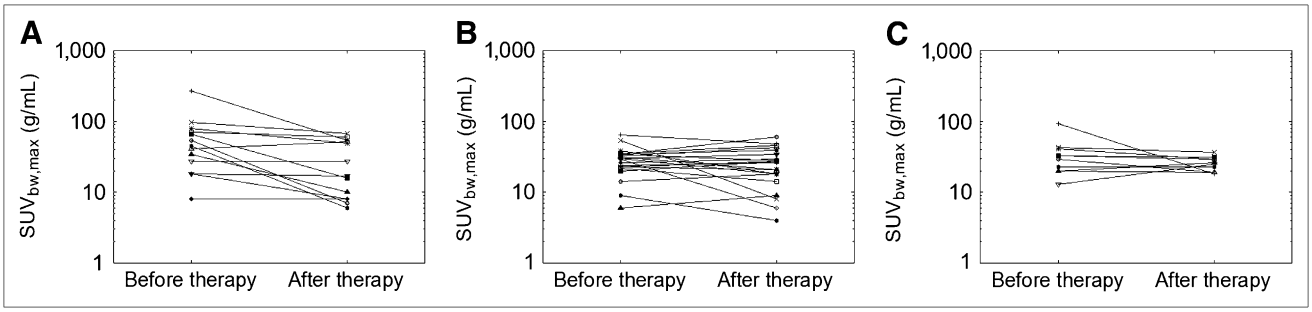


**FIGURE 5.** Relationship between clinical response and intrapatient changes in $^{18}$Ga-DOTA-TOC SUVs. Wilcoxon signed-rank test showed no significant difference in maximal SUV between pre- and posttherapy PET scans with noticeable variability among patients: clinical responders (A), patients with stable disease (B), and patients with progressive disease (C). $SUV_{bw,max}$ = maximal SUV normalized for body weight.

### Quantitative $^{68}$Ga-DOTA-TOC PET Analysis

A masked analysis of data was also conducted to calculate the SUV of individual target lesions. This cohort of patients showed a large range of intra- and interpatient SUV variability. According to our protocol, SUV was calculated for one and the same lesion in each patient. This analysis showed SUV to change rather randomly, so that no clear cutoff trend was evident and no clear correlation with outcome parameters was found. Neither initial SUV nor the percentage change in SUV during therapy, as indicated in Table 2, is a useful parameter for predicting patient outcome after PRRT.

There are several possible explanations for the overall variability in quantitative data. One is certainly the biologic tumor heterogeneity and the variable responsiveness of tumor tissue to radiation therapy (*12,25*). Furthermore, the fact that some patients were pretreated, for example, with chemotherapy, before being enrolled in the study could also have influenced the SSTR profile at the molecular level. The different time spans between final treatment and imaging might be another reason for SUV fluctuation. However, no significant differences in SUV were observed when patients with early restaging were compared 1 mo after therapy and 3 mo after therapy.

### Limitations of This Study

One limitation of the current analysis might be that different lesions were chosen for CT or MRI and $^{68}$Ga-DOTA-TOC PET analysis. However, choosing the same lesions for therapy evaluation would have meant defining a reference target lesion before assessing images, which would bias the masked reviewers. For this reason, a head-to-head comparison of PET and CT for the same index lesions was achieved in only 2 patients with stable disease.

Additionally, patients underwent a variable number of treatment cycles because of the individualized therapy protocol used at our department, which also includes dosimetric data and clinical parameters (*9*), reflecting a typical clinical situation.

## CONCLUSION

In contrast to staging of patients with SSTR-expressing tumors, in which $^{68}$Ga-DOTA-TOC PET is clearly superior to CT (*8*), there is little if any support for peptide receptor imaging with PET as a means of predicting therapy response. However, in addition to conventional imaging (CT), $^{68}$Ga-DOTA-TOC whole-body PET can be helpful as an early predictor of progressive disease by detecting new

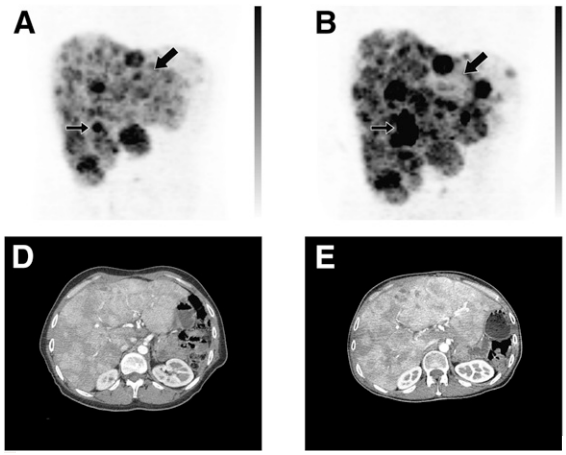


**FIGURE 6.** A 34-y-old man (patient 17) with disseminated liver metastases of neuroendocrine pancreatic tumor (A). After 4 cycles of $^{90}$Y-DOTA-TOC, his clinical condition indicated progressive disease although 1 large liver lesion (large arrow) showed decreased uptake on follow-up PET (B). However, $^{18}$F-FDG PET revealed enhanced uptake in this lesion (C), and a process of further dedifferentiation was thus assumed. Tumor progression was also confirmed with diagnostic CT (before therapy [D] and after therapy [E]). Retention of tracer in renal calices of right kidney shines through as indicated by small arrow.

metastases that developed during therapy. Evaluation of individual lesions, that is, diameter according to RECIST or SUV analysis, has been shown to be of no clinical value.

## REFERENCES


1. Van Essen M, Krenning EP, De Jong M, Valkema R, Kwekkeboom DJ. Peptide receptor radionuclide therapy with radiolabelled somatostatin analogues in patients with somatostatin receptor positive tumours. *Acta Oncol.* 2007;46:723–734.
2. Kwekkeboom DJ, Teunissen JJ, Bakker WH, et al. Radiolabeled somatostatin analog [$^{177}$Lu-DOTA0,Tyr3]octreotate in patients with endocrine gastropancreatic tumors. *J Clin Oncol.* 2005;23:2754–2762.
3. Teunissen JJ, Kwekkeboom DJ, Krenning EP. Quality of life in patients with gastroenteropancreatic tumors treated with [$^{177}$Lu-DOTA0,Tyr3]octreotate. *J Clin Oncol.* 2004;22:2724–2729.
4. Quaedvlieg PF, Visser O, Lamers CB, Janssen-Heijen ML, Taal BG. Epidemiology and survival in patients with carcinoid disease in The Netherlands: an epidemiological study with 2,391 patients. *Ann Oncol.* 2001;12:1295–1300.
5. Modlin IM, Lye KD, Kidd M. A 5-decade analysis of 13,715 carcinoid tumors. *Cancer.* 2003;97:934–959.
6. Friedberg JW, Van den Abbeele AD, Kehoe K, Singer S, Fletcher CD, Demetri GD. Uptake of radiolabeled somatostatin analog is detectable in patients with metastatic foci of sarcoma. *Cancer.* 1999;86:1621–1627.
7. Faiss S, Pape UF, Bohmig M, et al. Prospective, randomized, multicenter trial on the antiproliferative effect of lanreotide, interferon alfa, and their combination for therapy of metastatic neuroendocrine gastroenteropancreatic tumors—the International Lanreotide and Interferon Alfa Study Group. *J Clin Oncol.* 2003; 21:2689–2696.
8. Gabriel M, Decristoforo C, Kendler C, et al. $^{68}$Ga-DOTA-Tyr3-octreotide PET in neuroendocrine tumors: comparison with somatostatin receptor scintigraphy and CT. *J Nucl Med.* 2007;48:508–518.
9. Gabriel M, Andergassen U, Putzer D, et al. Innsbruck experience with targeted radionuclide therapy using different radiolabeled somatostatin analogs [abstract]. *Eur J Nucl Med Mol Imaging.* 2007;34(suppl 2):S220.
10. Therasse P, Arbuck SG, Eisenhauer EA, et al. New guidelines to evaluate the response to treatment in solid tumors. European Organization for Research and Treatment of Cancer, National Cancer Institute of the United States, National Cancer Institute of Canada. *J Natl Cancer Inst.* 2000;92:205–216.
11. Oberg K, Jelic S; ESMO Guidelines Working Group. Neuroendocrine gastroenteropancreatic tumors: ESMO clinical recommendations for diagnosis, treatment and follow-up. *Ann Oncol.* 2008;19(suppl 2):ii104–ii105.
12. Koukouraki S, Strauss LG, Georgoulias V, et al. Evaluation of the pharmacokinetics of $^{68}$Ga-DOTATOC in patients with metastatic neuroendocrine tumours scheduled for $^{90}$Y-DOTATOC therapy. *Eur J Nucl Med Mol Imaging.* 2006;33: 460–466.
13. Decristoforo C, Knopp R, von Guggenberg E, et al. A fully automated synthesis for the preparation of $^{68}$Ga-labelled peptides. *Nucl Med Commun.* 2007;28:870–875.
14. Krenning EP, Valkema R, Kwekkeboom DJ, et al. Molecular imaging as in vivo molecular pathology for gastroenteropancreatic neuroendocrine tumors: implications for follow-up after therapy. *J Nucl Med.* 2005;46(suppl):76S–82S.
15. Frilling A, Weber F, Saner F, et al. Treatment with $^{90}$Y- and $^{177}$Lu-DOTATOC in patients with metastatic neuroendocrine tumors. *Surgery.* 2006;140:968–976.
16. Forrer F, Waldherr C, Maecke HR, Mueller-Brand J. Targeted radionuclide therapy with $^{90}$Y-DOTATOC in patients with neuroendocrine tumors. *Anticancer Res.* 2006;26:703–707.
17. Bodei L, Cremonesi M, Grana C, et al. Receptor radionuclide therapy with $^{90}$Y-[DOTA]0-Tyr3-octreotide ($^{90}$Y-DOTATOC) in neuroendocrine tumours. *Eur J Nucl Med Mol Imaging.* 2004;31:1038–1046.
18. Forrer F, Uusijärvi H, Storch D, Maecke HR, Mueller-Brand J. Treatment with $^{177}$Lu-DOTATOC of patients with relapse of neuroendocrine tumors after treatment with $^{90}$Y-DOTATOC. *J Nucl Med.* 2005;46:1310–1316.
19. Waldherr C, Pless M, Maecke HR, et al. Tumor response and clinical benefit in neuroendocrine tumors after 7.4 GBq $^{90}$Y-DOTATOC. *J Nucl Med.* 2002;43:610–616.
20. Gabriel M, Hausler F, Bale R, et al. Image fusion analysis of $^{99m}$Tc-HYNIC-Tyr$^3$-octreotide SPECT and diagnostic CT using an immobilization device with external markers in patients with endocrine tumours. *Eur J Nucl Med Mol Imaging.* 2005;32:1440–1451.
21. Pfannenberg AC, Aschoff P, Brechtel K, et al. Value of contrast-enhanced multiphase CT in combined PET/CT protocols for oncological imaging. *Br J Radiol.* 2007;80:437–445.
22. Belhocine T, Foidart J, Rigo P, et al. Fluorodeoxyglucose positron emission tomography and somatostatin receptor scintigraphy for diagnosing and staging carcinoid tumours: correlations with the pathological indexes p53 and Ki-67. *Nucl Med Commun.* 2002;23:727–734.
23. Kayani I, Bomanji JB, Groves A, et al. Functional imaging of neuroendocrine tumors with combined PET/CT using $^{68}$Ga-DOTATATE (DOTA-DPhe1,Tyr3-octreotate) and $^{18}$F-FDG. *Cancer.* 2008;112:2447–2455.
24. Lebtahi R, Cadiot G, Delahaye N, et al. Detection of bone metastases in patients with endocrine gastroenteropancreatic tumors: bone scintigraphy compared with somatostatin receptor scintigraphy. *J Nucl Med.* 1999;40:1602–1608.
25. Koukouraki S, Strauss L, Georgoulias V, Eisenhut M, Haberkorn U, Dimitrakopoulou-Strauss A. Comparison of the pharmacokinetics of $^{68}$Ga-DOTA-TOC and [$^{18}$F]FDG in patients with metastatic neuroendocrine tumours scheduled for $^{90}$Y-DOTA-TOC therapy. *Eur J Nucl Med Mol Imaging.* 2006;33:1115–1122.

JNM The Journal of NUCLEAR MEDICINE

# $^{68}$Ga-DOTA-Tyr$^{3}$-Octreotide PET for Assessing Response to Somatostatin-Receptor–Mediated Radionuclide Therapy

Michael Gabriel, Andreas Oberauer, Georg Dobrozemsky, Clemens Decristoforo, Daniel Putzer, Dorota Kendler, Christian Uprimny, Peter Kovacs, Reto Bale and Irene J. Virgolini

*J Nucl Med.* 2009;50:1427-1434.
Published online: August 18, 2009.
Doi: 10.2967/jnumed.108.053421



*The Journal of Nuclear Medicine* is published monthly.
SNMMI | Society of Nuclear Medicine and Molecular Imaging
1850 Samuel Morse Drive, Reston, VA 20190.
(Print ISSN: 0161-5505, Online ISSN: 2159-662X)



SNMMI SOCIETY OF NUCLEAR MEDICINE AND MOLECULAR IMAGING